[2] Felippa, C. A. and Clough, R. W., "The Finite Element Method in Solid Mechanics," *Proceedings of the Symposium on Numerical Solutions of Field Problems in Continuum Mechanics,* American Mathematical Society, Providence, R. I., April 1968.

[3] Walz, J. E., Fulton, R. E., and Cyrus, N. J., "Accuracy and Convergence of Finite Element Approximations," *Proceedings of the 2nd Conference on Matrix Methods in Structural Mechanics,* AFFDL-TR-68-150, Air Force Flight Dynamics Lab., Wright-Patterson Air Force Base, Ohio, 1968.

[4] Oden, J. T. and Brauchli, H. J., "A Note on Accuracy and Convergence of Finite Element Approximations," *International Journal for Numerical Methods in Engineering,* Vol. 3, 1971, pp. 291–292.

[5] Murray, K. H., "Comments on the Convergence of Finite Element Solutions," *AIAA Journal,* Vol. 8, No. 4, April 1970, pp. 815–816.

[6] Jones, R. E. and Strome, D. R., "Direct Stiffness Method Analysis of Shells of Revolution Utilizing Curved Elements," *AIAA Journal,* Vol. 4, No. 9, Sept. 1966, pp. 1519–1525.

[7] Stricklin, J. A., Navaratna, D. R., and Pian, T. H. H., "Improvements on the Analysis of Shells of Revolution by the Matrix Displacement Method," *AIAA Journal,* Vol. 4, No. 11, Nov. 1966, pp. 2069–2072.

[8] Adelman, H. M., Catherines, D. S., and Walton, W. C., "Accuracy of Modal Stress Calculations by the Finite Element Method," *AIAA Journal,* Vol. 8, No. 3, March 1970, pp. 462–468.

[9] Mebane, P. M. and Stricklin, J. A., "Implicit Rigid Body Motion in Curved Finite Elements," *AIAA Journal,* Vol. 9, No. 2, Feb. 1971, pp. 344–345.

[10] Gallagher, R. H., "Analysis of Plate and Shell Structures," *Proceedings of the Symposium on Application of Finite Element Methods in Civil Engineering,* Vanderbilt Univ., Nashville, Tenn., 1969.

[11] Haisler, W. E. and Stricklin, J. A., "Rigid-Body Displacements of Curved Elements in the Analysis of Shells by the Matrix-Displacement Method," *AIAA Journal,* Vol. 5, No. 8, Aug. 1967, pp. 1525–1527.

[12] Bogner, F. K., Fox, R. L., and Schmit, L. A., "A Cylindrical Shell Discrete Element," *AIAA Journal,* Vol. 5, No. 4, April 1967, pp. 745–750.

[13] Schmit, L. A., Bogner, F. K., and Fox, R. L., "Finite Deflection Structural Analysis Using Plate and Shell Discrete Elements," *AIAA Journal,* Vol. 6, No. 5, May 1968, pp. 781–791.

[14] Cantin, G. and Clough, R. W., "A Curved, Cylindrical-Shell, Finite Element," *AIAA Journal,* Vol. 6, No. 6, June 1968, pp. 1057–1062.

[15] Fonder, G. A., "A Doubly Curved Quadrilateral Element for Thin Elastic Shells of Revolution," Ph.D. dissertation, Jan. 1972, Dept. of Civil Engineering, Univ. of California, Berkeley.

[16] Cantin, G., "Strain Displacement Relationships for Cylindrical Shells," *AIAA Journal,* Vol. 6, No. 9, Sept. 1968, pp. 1787–1788.

[17] Koiter, W. T., "A Consistent First Approximation in the General Theory of Thin Elastic Shells," *Proceedings of IUTAM Symposium on the Theory of Thin Elastic Shells,* edited by W. T. Koiter, North Holland, Amsterdam, 1960.

[18] Sanders, J. L., "An Improved First Approximation Theory for Thin Shells," Rept. 24, June 1959, NASA.

[19] Bogner, F. K., Fox, R. L., and Schmit, L. A., "The Generation of Interelement-Compatible Stiffness and Mass Matrices by the Use of Interpolation Formulas," *Proceedings of the Conference on Matrix Methods in Structural Mechanics,* TR-66-80, Air Force Flight Dynamics Lab., Wright-Patterson Air Force Base, Ohio, 1966.

[20] Cantin, G., "Rigid Body Motions in Curved Finite Elements," *AIAA Journal,* Vol. 8, No. 7, July 1970, pp. 1252–1255.

[21] Clough, R. W. and Johnson, C. P., "Finite Element Analysis of Arbitrary Thin Shells," *Proceedings of the ACI Symposium on Concrete Thin Shells,* ACI Publication SP-28, 1971.

[22] Lee, T. M., "Flexure of Circular Plate by Concentrated Force," *Journal of Engineering Mechanics Division ASCE,* 96, EM3, pp. 841–855.

[23] Key, S. W., "The Analysis of Thin Shells with a Doubly Curved Arbitrary Quadrilateral Finite Element," *Proceedings of the Conference on Computer Oriented Analysis of Shells,* Lockheed Palo Alto Research Lab., Palo Alto, Calif., 1970.

[24] Larsen, P., "Large Displacements Analysis of Shells of Revolution Including Creep, Plasticity and Viscoelasticity," Ph.D. dissertation, 1972, Dept. of Civil Engineering, Univ. of California, Berkeley.

MARCH 1973 AIAA JOURNAL VOL. 11, NO. 3

Estimation of Control Surface Dynamic Derivatives from Flight Test Data

B. M. HALL,* M. S. SHOLAR,† AND A. P. ALLRED‡
McDonnell Douglas Astronautics Company—West, Huntington Beach, Calif.

A method is presented for estimating dynamic hinge moment coefficients of trailing-edge control surfaces from measurements of system states. The hinge moment coefficient expansion as a polynomial in reduced frequency is validated by wind-tunnel data for Mach numbers 0, 0.5, 1.0, and 1.2. Augmentation of system equations with the hinge moment coefficient expansion leads to finite-difference equations applicable to a discrete set of measurement data. Accurate estimates of hinge moment coefficients for a flapping wing-aileron model have been obtained by a parameter space search algorithm that minimizes the squared error between the estimated and measured control surface deflection. The estimating was performed by the digital portion of a hybrid computer operating on data from an analog simulation of a subsonic aileron. A most promising result is that the addition of noise on the measurements and errors in the system parameters did not notably degrade the estimation accuracy.

Nomenclature

b = semichord of wing
C = chord of wing, ft
C_δ = aileron chord, ft
$C_{h\delta}$ = dynamic hinge moment coefficient, per rad
$C_{h\delta 0}$ = static value of hinge moment coefficient, per rad
C_{Lz} = wing lift derivative, per rad
$C_{L\delta}$ = wing lift derivative due to aileron deflection
F = error function
I_δ = aileron moment of inertia, lb sec^2 ft
I_0 = wing moment of inertia about root, lb sec^2 ft
i = ith sample interval, incremental subscript
j = incremental subscript, $(-1)^{1/2}$
K = $C_{h\delta 0}$
k = incremental subscript
l = distance from root to center of aileron, ft
N = number of sampled points

Presented as Paper 72-379 at the AIAA/ASME/SAE 13th Structures, Structural Dynamics, and Materials Conference, San Antonio, Texas, April 10–12, 1972; submitted April 27, 1972; revision received October 2, 1972.

Index categories: Aircraft Vibration; Aircraft Handling, Stability, and Control.

* Chief, Flight Control Systems Branch. Associate Fellow AIAA.
† Senior Staff Engineer, Flight Control Systems Branch.
‡ Engineer Scientist, Simulations Systems.

P_δ = unbalance of aileron, positive tail heavy, lb sec^2
q = dynamic pressure, lb/ft^2
R_w = radius of gyration of wing, ft (with respect to the wing root)
S_w = total wing area, ft^2
S_δ = aileron area, ft^2
s = Laplace transform variable
T = sample interval
v = velocity of wing
y = dummy variable in Simpson integration
δ = aileron deflection, radians, positive tail down
δ_c = commanded aileron deflection
ζ = ratio of aileron damping due to servo to critical damping
τ = constants
τ_l = polynomial coefficient for digital reconstruction of $C_{h\delta}$
τ_i' = polynomial coefficients for analog model
ϕ = wing generalized deflection positive wing tip down
ω = angular frequency, rad/sec
ω_δ = aileron servo resonance, rad/sec
ω_B = bending frequency, rad/sec

Introduction

CONTROL surface dynamic hinge moment coefficients have presented a challenging problem to the theoretical aerodynamicists, as well as to the experimental aerodynamicists, for many years. Although the measurement of the static hinge moment characteristics of a control surface is relatively straightforward, at higher frequencies it is usually performed by oscillating control surfaces in sinusoidal motion throughout the frequency region of interest. This is a relatively difficult operation and requires the determination of in-phase and quadrature components of hinge moment, which presents major instrumentation and data reduction problems. The theoretical calculation of control surface hinge moments is, in a sense, a more amenable problem because one may start with a series of assumptions and laboriously crank through the solutions. The answers, however, do not, in general, agree well with the experimental data and have frequently failed to predict such phenomena as control surface buzz and single-degree-of-freedom flutter. In the past, aircraft control surface designs have been rendered free from flutter by mass balancing and providing sufficient actuator stiffness. In the future, there will be requirements for implementing the control of flutter by a feedback control system operating the control surface actuator. These same actuators will also be required to provide stability for control-configured vehicles and to provide automatic load relief systems in order to save structural weight. For this purpose it will be essential to have more accurate information on the dynamic characteristics of control surface hinge moments because the designer must now provide stability throughout the flight regime with the restraint that the control system must have a sufficiently high gain to provide control of flutter, loads, and rigid body stability. With these high gains the control systems engineer must have better information as to the high-frequency lags in his system in order that he be able to design the appropriate compensation networks and prescribe the servo parameters. The high-frequency phase margin against instability might well be only 20°–30°, and this in itself could be entirely used up by the uncertainty in dynamic hinge moment coefficient data. Many of these practical control system design problems were thoroughly reviewed in four papers presented at the 1971 Joint Automatic Control Conference. These papers dealt with B-52 and XB-70 flight test programs, as well as some work in progress on the F4 fighter aircraft. See Refs. 1–4.

The purpose of this paper is to present a method for the determination of the dynamic hinge moment coefficients from measurement of system states responding to a control servo command.

Basic Approach

The first step in the determination of the hinge moment coefficients is to make use of the fact that the hinge moment coefficient may be readily expanded as a polynomial in the reduced frequency, $\omega b/v$. The next step is to arrange the dynamic equations of the wing and the control surface so that the unknown coefficients of the polynomial appear as parameters in the equations and the systems states in the equation are measured values. The third step is to establish the error criterion which compares the estimated value of control surface deflection to the measured value. The estimated value in this case will be that which is obtained by solution of the system equations with trial values of the polynomial coefficients. The final step in this process is to iterate on these coefficients until the square of the error is minimized. The values of polynomial coefficients which result in this minimum value can then be substituted into the polynomial, and the hinge moment computed as a function of frequency. It is important to note that throughout the analysis it is assumed that the static value of hinge moment coefficient is known from previous wind-tunnel test data.

Control Surface Hinge Moment Representation

Before proceeding with the details of this estimation technique, it is necessary to investigate very briefly the mathematical form which is suitable for representation of the control surface hinge moments. Consider the hinge moment equation for a control surface.

$$\text{Hinge moment} = -qC_{h\delta}S_\delta C_\delta \delta \tag{1}$$

Equation (1a) shows that $C_{h\delta}$ may be approximated with a rather simple polynomial in reduced frequency. A steady-state sinusoidal motion and a $C_{h\delta}$ that varies as a function of frequency are assumed.

$$C_{h\delta} = C_{h\delta 0}\frac{[(1+j\tau_1\omega b/v)(1+j\tau_2\omega b/v)]}{1+\tau_3 j\omega b/v} \tag{1a}$$

where the τ's are constant for any Mach number and angle of attack for which it is desired to determine $C_{h\delta}$ experimentally.

This form for representing unsteady aerodynamics is, of course, not new; it has been used for many years to characterize the lag functions in unsteady aerodynamics which are necessary for transient loads analysis. In arriving at the polynomial form of this model valid at low frequencies, it is desired to achieve as simple an expression as possible but still retain the characteristics necessary to describe the real physical phenomena. This expansion satisfies these requirements by reducing to a constant known value at zero frequency and by providing the phase lag necessary to describe single-degree-of-freedom flutter phenomena. In order to justify this polynomial, the theoretical and experimental characteristics of a trailing-edge aileron whose leading edge is located at the 75% chord from the wing leading edge are examined. Figure 1 shows this aileron hinge moment as computed from Ref. 5.

The polynomial fits the data extremely well up to a reduced frequency of 1.0. For the high frequencies ($\omega b/v > 2$) the apparent mass of air surrounding the control surface dominates the

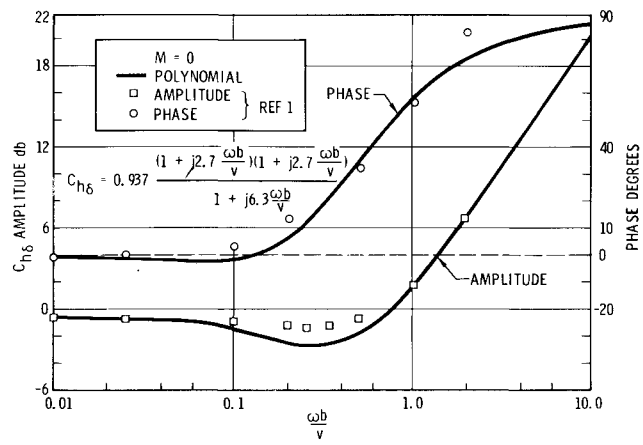

Fig. 1 Approximation to strip theory, $M = 0$.

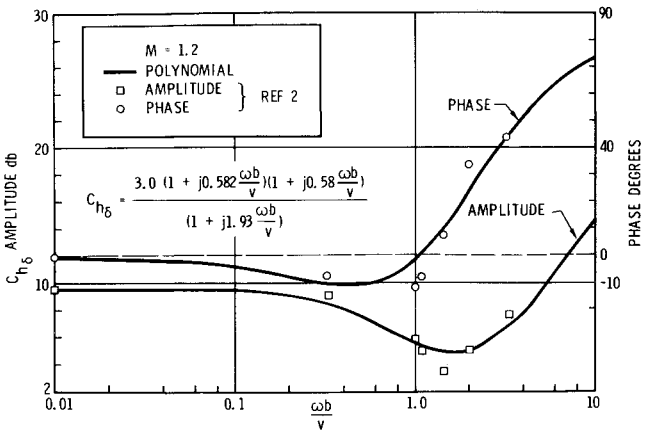

Fig. 2 Approximation to strip theory, $M = 1.2$.

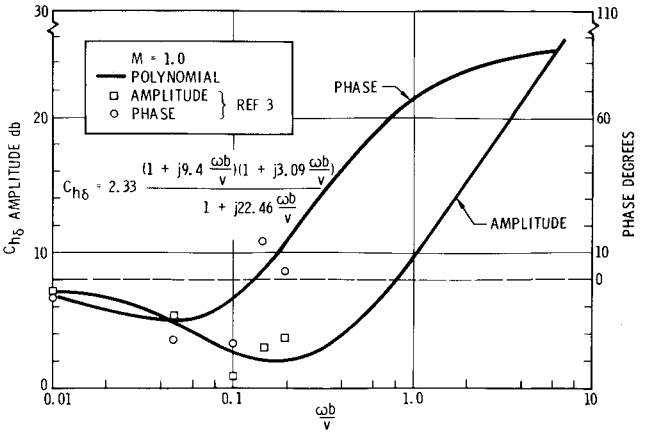

Fig. 4 Approximation to test data, $M = 1.0$.

dynamic response, and the hinge moment characteristic increases at 12 db per octave. This very high-frequency region is of little general interest to the servo designer. Figure 2 shows a similar hinge moment characteristic taken from Ref. 6.

For Mach numbers greater than 2, piston theory is applicable in many cases. For piston theory the hinge moment takes on a very simple dynamic form, as shown below

$$C_{h\delta} = (2/M)[1 + (j/3)\omega b/v] \tag{1b}$$

In this case, it is necessary to consider the estimation of only the single coefficient, τ_1, in the polynomial form.

As an example of the experimental data available, Figs. 3 and 4 show a very limited number of experimental points taken from Ref. 7. Although the curve fit in this case certainly is not good throughout the frequency range, it is reasonable to assume that the data should be well behaved over a finite frequency interval, and that the erratic nature of the test points is due to experimental error. Figures 1–4 show negative phase angles, indicating the possibility of single-degree-of-freedom control surface flutter.

Application to an Airframe Model

Although the technique presented in this paper is applicable to a general flexible airframe, the most expedient way to understand the technique is to consider a specific example such as the flapping wing aileron model shown in Fig. 5.

The equations of motion for this model are as follows:

$$\ddot{\delta} = -l\ddot{\phi}P_\delta/I_\delta - C_{h\delta}qS_\delta C_\delta\delta/I_\delta - \omega_\delta{}^2\delta - 2\zeta\omega_\delta\dot{\delta} + \ddot{\delta}_c \tag{2}$$

$$\ddot{\phi} = -qS_w C_{L\delta}l\delta/I_0 - C_{Lx}S_w qR_w{}^2\dot{\phi}/I_0 v - \omega_B{}^2\phi - lP_\delta\ddot{\delta}/I_0 \tag{2a}$$

This model was chosen because it is complex enough to serve as a practical example, yet simple enough to prevent obscuring the basic estimation details. This model contains the following basic assumptions: a) $C_{L\delta}$ and C_{Lx} are known static values; b) the real part of lift on the wing due to wing plunging is neglected; c) the quadrature component (imaginary part) of the wing lift due to aileron rotation is ignored; d) the aerodynamic moment on the aileron due to wing plunging is assumed to be small compared to the mass coupling between the wing and the aileron; and e) the aileron is driven by a servo of known characteristics.

It may be argued that C_{Lx} and $C_{L\delta}$ should be included in the estimation procedure and, indeed, this is a possibility. In the numerical example which follows it will be shown, however, that errors in these known values, for this example, do not affect the C_L estimation. It is assumed that ground tests will provide good values for inertia characteristics, servo characteristics, and wing bending. In conjunction with this model, it is assumed that the following measurements are available: a) aileron position, b) aileron rotation acceleration, and c) wing flapping acceleration (the wing itself is assumed to be rigid, but suspended by a clock spring at the root).

Error Function Criteria

The estimation technique can be very basically stated as follows: find the coefficients, τ_1, τ_2, and τ_3, so that the following function F is minimized:

$$F = \sum_{i=3}^{N} (\delta_i - \hat{\delta}_i)^2 \tag{3}$$

where $\hat{\delta}_i$ is the estimated value of δ_i at the ith time interval, and N is the number of time points sampled.

The purpose of this error function is to compare the control surface deflection, which is measured at the ith time interval, to that deflection which is estimated from the system equations with trial values of the polynomial coefficients. If these coefficients

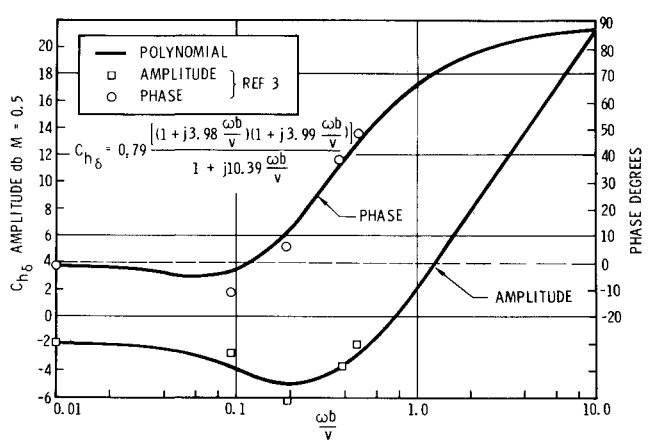

Fig. 3 Approximation to test data, $M = 0.5$.

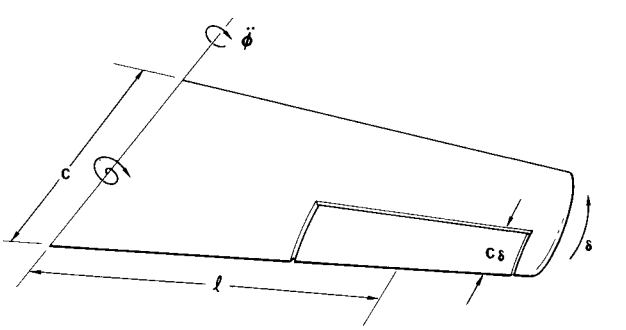

Fig. 5 Airframe model.

are approximately correct, the time history of the estimated δ and the measured δ will be approximately equal, and the error in these two functions, when summed over all N time points, will be small. If the error is large, the new values of the polynomial coefficients must be found in order to reduce the error. This process is repeated continuously until a set of polynomial coefficients is located which reduces the error function to a minimum.

Estimation Procedure

In order to implement this technique and produce a digital program, the following steps are taken:

A) Using the polynomial form for C_{h_δ} substitute the Laplace transform variable, s, for $j\omega$.

B) Substitute the polynomial form of C_{h_δ} in the aileron moment equation [Eq. (2)].

C) Multiply both sides of the equation by the denominator of C_{h_δ}, $(1+[b/v]\tau_3 s)$. This leaves the equation in terms of the measured states (δ, $\dot{\delta}$, $\dot{\phi}$), the derivative terms, $\ddot{\delta}$, $\dddot{\delta}$, and $\ddot{\phi}$, and the command $\ddot{\delta}_c$. The next steps are taken to eliminate the unmeasured terms, $\ddot{\delta}$, $\dddot{\delta}$, $\ddot{\phi}$, and $\ddot{\delta}_c$.

D) The odd-numbered derivatives are eliminated by grouping them on the left side of the equation. The measured, or even, derivatives are then grouped on the right side of the equation. Simpson's rule is then applied to integrate the left side of the equation in terms of the present value of the right side and the two previous values. Simpson's rule, as used here, is as follows:

$$Y_i = Y_{i-2}+(T/3)(\dot{Y}_{i-2}+4\dot{Y}_{i-1}+\dot{Y}_i) \tag{4}$$

This leaves the equation in terms of the measured states, δ, $\dot{\delta}$, and $\ddot{\phi}$, sampled at the ith time interval, as well as the sampled values of these states and the command acceleration at the two previous time intervals.

E) The final purely algebraic step is to solve for δ at the ith time interval in terms of δ at the two previous intervals, and in terms of $\dot{\delta}$, $\ddot{\phi}$, and $\ddot{\delta}_c$ at the two previous intervals. We shall call δ_i at the ith interval $\hat{\delta}_i$ (the estimated value).

F) The equations are now complete, and $\hat{\delta}_i$ and δ_i may be substituted into the error function, Eq. (3).

G) The iteration procedure for determining the polynomial coefficients is performed by assuming a value for each coefficient. An arbitrary increment above and below the assumed value is taken and the error function computed for all combinations of the perturbed value of the coefficients. This process is repeated by moving in the direction of each τ which leads to the smallest value of the error function.

Iteration Procedure

As with all parameter estimation techniques, the basic concepts for minimization are straightforward and deceptively simple to mechanize. In this particular case, a grid search on the polynomial coefficients is initiated, the error for all combinations of τ_1, τ_2, and τ_3 estimated, and the minimum value chosen. This process certainly does work and will yield reasonable results. However, the machine time required to compute the error function to construct this grid is prohibitive. Therefore, some method for estimating the values of the unknown coefficients must be chosen based on the information gained from the previous set of values. This, in essence, is the subject of a whole body of mathematical literature concerned with algorithms for solving minimization problems. In order not to digress from the basic subject of this paper, and because it is evident that this particular estimation problem does have solutions, only the computing algorithm which was successfully used for the example described in the Appendix is presented. Very briefly, the detailed steps in the Appendix may be described as a process in which an initial set of the polynomial coefficients, τ_1, τ_2, and τ_3, is chosen and the error function evaluated. Each τ is incremented in a cubical grid search pattern which, essentially, provides an estimate of the gradient direction. This process is repeated in successive steps with the step size reducing as the error function decreases. This decreases until an arbitrary minimum criterion is reached. There is always the problem of multiple minimum values; however, in the cases tried on the analog computer, the unknown aerodynamic functions were well behaved, and no trouble was encountered in finding the τ's in the desired region.

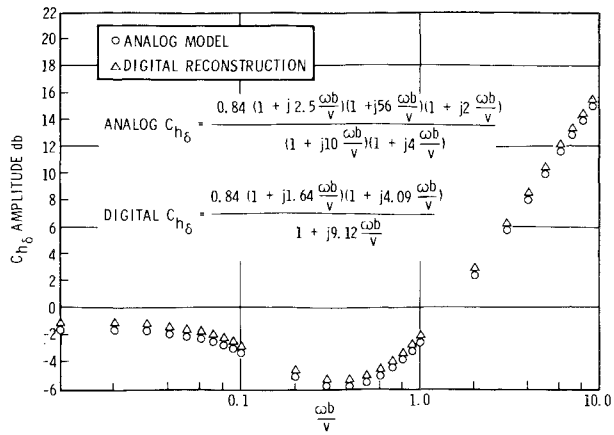

Fig. 6 C_{h_δ} **estimation, no noise case.**

Sample Problem

Referring to the system equations [Eqs. (2) and (2a)], numerical data will be substituted and how the process evolves demonstrated. In this particular case a hybrid computer system is utilized. This system consists of an XDS 930 digital computer and a Beckman 2200 analog computer. The analog computer is used to simulate the dynamic system, and the digital computer is used to sample the output of this system and form the computing algorithm for the unknown polynomial coefficients. The numerical data employed in this example are given in the Appendix. The analog system in this example contains somewhat more complex aerodynamics than assumed by the digital processor. This complication (an additional lag-lead) is employed because it is desirable to simulate a real case where the digital processor is only approximating a more complex aerodynamic system. Previous investigations on this type of system have shown that accurate results are achieved if the digital processor assumes a polynomial form which is an exact duplication of the form used in the model. In the practical case, of course, the actual aerodynamics of the model will not be known and, indeed, will probably not possess an exact polynomial representation of any degree. For this study the system is excited with an arbitrary input which is assumed to be known. The results shown in Fig. 6 are all from step inputs.

The technique was applied to the sample problem for the following cases: a) estimation of polynomial coefficients for no noise and all parameters known perfectly; b) estimation of polynomial coefficients for measurement noise on $\ddot{\phi}$ and $\dddot{\delta}$; and c) estimation of polynomial coefficients for error in the parameters of the system equations. Figure 6 shows the results of the first case.

The approximate aerodynamic representation used in the digital processor does a good job of approximating the more complex function used on the analog. The error in amplitude is less than 0.5 db, and the error in phase is less than 1°.

The purpose of the next series of runs is to investigate the effect of noise on the measurement of the states. For these runs an analog noise generator was used, which produced zero-mean white noise. This noise was passed through a filter which rolled off the high frequencies at 6 db per octave above $\omega b/v = 12.5$. This is the type of filter which would normally be found in any practical instrumentation system. The results of these noise runs are summarized in Table 1.

Table 1 Effect of noise

% noise on $\ddot{\phi}$	% noise on $\ddot{\delta}$	Max amp. error, db	Max phase error, deg
0	0	<0.5	<1.0
4	0	<0.5	<1.0
6	0	<0.5	<1.0
20	0	<0.5	1.7
0	2	0.8	3.0
0	4	1.8	7.4

Noise measurements do cause error in the estimation of polynomial coefficients. Although this type of error is to be expected, a carefully designed instrumentation system should not pick up noise levels which significantly affect the output. The percent of noise is calculated by setting the rms noise level to a specified percent of 0.7 times the zero-to-peak maximum signal level of the state.

The important point is that this system functions properly even though noise measurements are present. Noise could not be superimposed upon more than one state at a time because only one noise generator was available for this study. It is anticipated that noise on the other states would not seriously affect the parameter estimation providing the noise signals are not correlated.

As an additional test on this system, several parameters were mismatched between the digital processor and the analog computer. The results are summarized in Table 2.

Table 2, as expected, shows that errors in parameters which are assumed to be known certainly affect the results to a greater or lesser degree depending upon the critical nature of the mismatched parameters. As with all numerical examples, the results with respect to the chosen numerical values must be considered. In this particular example, the system is relatively insensitive to noise on the wing bending measurements and to error in the calculation of mass unbalance. The reason for this is that there is a relatively small amount of mass unbalance in this case. Also, surprisingly large uncertainties in servo damping can be tolerated without large errors. This is probably due to the fact that the servo was chosen to have an open-loop damping of only 10%. If the servo has a very large value of open-loop damping, it would contribute to large errors in phase uncertainty of the hinge moment coefficients, although this parameter was not investigated in detail. Uncertainty in the static hinge moment coefficient causes significant variation in the hinge moment coefficient estimation. This, too, is to be expected, but this problem should be overcome by careful static hinge moment measurements performed in the wind tunnel. As an additional test on the system, plant noise was introduced as a random disturbance producing a hinge moment. The results are similar to noisy measurements on $\ddot{\delta}$. Unknown disturbances do affect the estimate of polynomial coefficients, and the experiment should be performed in a manner to minimize these unknown disturbances and, hence, arrive at the best possible estimate of the polynomials for the hinge moment.

The important conclusion is that the method still converges and arrives at a reasonable polynomial approximation for the aerodynamic functions. The computer run-time for achieving a converged value of polynomial coefficients varies depending upon whether there is a noise in the system but, in general, the run-times were on the order of 20 min. This method in general is not adaptable for on-line estimation because of the iterative approach and rather long computer run-time. This, however, is not a serious drawback since the method will find its greatest use in wind tunnel data reduction and inflight data reduction. For both of these cases, the data are normally stored on magnetic tapes for later processing.

Table 2 Effect of parameter variation

Parameter variation	Max amp. error, db	Max phase error, deg
All parameters known exactly	<0.5	<1.0
10% error in $P_{\ddot{\delta}}$, mass unbalance	<0.5	<1.0
30% error in $P_{\ddot{\delta}}$	<0.5	1.2
10% error in ζ, servo damping	<0.5	<1.0
30% error in ζ	0.8	3.1
10% error in $C_{h\ddot{\delta}0}$, static hinge moment	1.3	3.7
20% error in $C_{h\ddot{\delta}0}$	2.5	8.2

Conclusions

This paper has presented a method for estimating the dynamic hinge moment characteristics of trailing-edge control surfaces. Although the technique is applied to a relatively simple system, the variation of parameters and introduction of noise have created a practical situation which permits more faith to be placed in the method. There will undoubtedly be other problems associated with the processing of data from real flexible models or flight aircraft, but the noise scheme presented here should be applicable to these more complex situations.

Appendix

The parameters for the model in Fig. 5 are shown in Table 3. Substituting the values in Table 3 into Eq. (2) (aileron equation) and carrying out the algebraic manipulations outlined in the Error Function Criteria paragraph, the following equations are obtained.

Filter Equations

$$\ddot{\delta} = -0.21\ddot{\phi} - \frac{v^2}{400}K\left(1+\tau_1\frac{10}{v}s\right)\frac{[1+\tau_2(10/v)s]}{[1+\tau_3(10/v)s]}\delta - \omega_\delta{}^2\delta - 2\zeta\omega_\delta\dot{\delta} + \ddot{\delta}_c \qquad \text{(A1)}$$

$$\ddot{\delta} + \tau_3\frac{10}{v}\dddot{\delta} = -0.21\ddot{\phi} - 0.21\tau_3\frac{10}{v}\dddot{\phi} - \frac{Kv^2}{400}\delta - \frac{Kv}{40}(\tau_1+\tau_2)\dot{\delta} - 0.25K\tau_1\tau_2\ddot{\delta} + \ddot{\delta}_c + \tau_3\frac{10}{v}\dddot{\delta}_c - \omega_\delta{}^2\delta - \tau_3\frac{10}{v}\omega_\delta{}^2\dot{\delta} - 2\zeta\omega_\delta\ddot{\delta} - 2\tau_3\frac{10}{v}\zeta\omega_\delta\dddot{\delta} \qquad \text{(A2)}$$

Table 3 Parameter values for the model in Fig. 5

Parameter	Value
AR	5
Aileron leading edge	75% of chord from wing leading edge
Velocity	400 fps
ω_B	10 rad/sec
ω_δ	5 rad/sec
$\frac{lP_\delta}{I_\delta}$	0.21 (tail heavy aileron)
$\frac{qS_\delta C_\delta}{I_\delta}$	$\frac{v^2}{400}$ 1/sec^2
ζ	0.1
$\frac{qS_w C_{L\delta} l}{I_0}$	35.8 1/sec^2
$\frac{C_{Lz} S_w q R_w{}^2}{I_0 v}$	6 1/sec
$\frac{lP_\delta}{I_0}$	7.7×10^{-5}
b	Semichord = 10 ft
T	Sample interval = 0.01 sec

$$\tau_3\frac{10}{v}\dddot{\delta}+0.21\tau_3\frac{10}{v}\ddot{\phi}+\frac{Kv}{40}(\tau_1+\tau_2)\ddot{\delta}-\tau_3\frac{10}{v}\dddot{\delta}_c+$$
$$\tau_3\frac{10}{v}\omega_\delta{}^2\dot{\delta}+2\zeta\omega_\delta\ddot{\delta}=-0.21\ddot{\phi}-\frac{Kv^2}{400}\delta-$$
$$0.25K\tau_1\tau_2\ddot{\delta}-\dot{\delta}+\ddot{\delta}_c-\omega_\delta{}^2\delta-2\tau_3\frac{10}{v}\zeta\omega_\delta\dot{\delta} \qquad \text{(A3)}$$

Integrate Eq. (A3) using Simpson's rule:

$$Y_{i+2}=Y_i+(T/3)(Y_i'+4Y_{i+1}+Y_{i+2}')$$
$$\tau_3\frac{10}{v}\ddot{\delta}_{i+2}+0.21\tau_3\frac{10}{v}\ddot{\phi}_{i+2}+\frac{Kv}{40}(\tau_1+\tau_2)\delta_{i+2}-$$
$$\tau_3\frac{10}{v}\ddot{\delta}_{ci+2}+\tau_3\frac{10}{v}\omega_\delta{}^2\delta_{i+2}+2\zeta\omega_\delta\delta_{i+2}=$$
$$\tau_3\frac{10}{v}\ddot{\delta}_i+0.21\tau_3\frac{10}{v}\ddot{\phi}_i+\frac{Kv}{40}(\tau_1+\tau_2)\delta_i-\tau_3\frac{10}{v}\ddot{\delta}_{ci}+$$
$$\tau_3\frac{10}{v}\omega_\delta{}^2\delta_i+2\zeta\omega_\delta\delta_i-0.21(T/3)(\ddot{\phi}_i+4\ddot{\phi}_{i+1}+\ddot{\phi}_{i+2})-$$
$$\frac{Kv^2}{1200}T(\delta_i+4\delta_{i+1}+\delta_{i+2})-\frac{0.25KT}{3}\tau_1\tau_2(\ddot{\delta}_i+4\ddot{\delta}_{i+1}+\ddot{\delta}_{i+2})-$$
$$(T/3)(\ddot{\delta}_i+4\ddot{\delta}_{i+1}+\ddot{\delta}_{i+2})+(T/3)(\ddot{\delta}_{ci}+4\ddot{\delta}_{ci+1}+\ddot{\delta}_{ci+2})-$$
$$\omega_\delta{}^2(T/3)(\delta_i+4\delta_{i+1}+\delta_{i+2})-2\tau_3\frac{10}{v}\zeta\omega_\delta(T/3)\times$$
$$(\ddot{\delta}_i+4\ddot{\delta}_{i+1}+\ddot{\delta}_{i+2}) \qquad \text{(A4)}$$

Solve for: $\hat{\delta}_{1+2}$

$$\hat{\delta}_{i+2}\left[\frac{Kv^2T}{1200}+\omega_\delta{}^2T/3+2\zeta\omega_\delta+\tau_3\frac{10}{v}\omega_\delta{}^2+(\tau_1+\tau_2)\frac{Kv}{40}\right]=$$
$$2\zeta\omega_\delta\delta_i-\omega_\delta{}^2(T/3)(\delta_i+4\delta_{i+1})-$$
$$0.21(T/3)(\ddot{\phi}_i+4\ddot{\phi}_{i+1}+\ddot{\phi}_{i+2})-\frac{Kv^2T}{1200}(\delta_i+4\delta_{i+1})-$$
$$(T/3)(\ddot{\delta}_i+4\ddot{\delta}_{i+1}+\ddot{\delta}_{i+2})+(T/3)(\ddot{\delta}_{ci}+4\ddot{\delta}_{ci+1}+\ddot{\delta}_{ci+2})+$$
$$\tau_3\frac{10}{v}[\ddot{\delta}_i-\ddot{\delta}_{i+2}+0.21(\ddot{\phi}_i-\ddot{\phi}_{i+2})]+[\ddot{\delta}_{ci+2}-\ddot{\delta}_{ci}+\omega_\delta{}^2\delta_i-$$
$$2\zeta\omega_\delta(T/3)(\ddot{\delta}_i+4\ddot{\delta}_{i+1}+\ddot{\delta}_{i+2})]\tau_3\frac{10}{v}+(\tau_1+\tau_2)\frac{Kv}{40}\delta_i-$$
$$0.25\tau_1\tau_2\frac{KT}{3}(\ddot{\delta}_i+4\ddot{\delta}_{i+1}+\ddot{\delta}_{i+2}) \qquad \text{(A5)}$$

Minimize τ_1, τ_2, τ_3:

$$F=\sum_{i=3}^{N}(\delta_1-\hat{\delta}_i)^2$$

Minimization Procedure

1) Specify initial values for

$$\tau_1{}^0, \tau_2{}^0, \tau_3{}^0, \Delta\tau_1, \Delta\tau_2, \Delta\tau_3$$

2) Evaluate error

$$(\tau_1, \tau_2, \tau_3)=\sum_{m=3}^{N}(\delta_m-\hat{\delta}_m)^2$$

at the following points:

$$\text{Error}(i,j,k)=\text{Error}(\tau_1{}^n+i\Delta\tau_1{}^n, \tau_2{}^n+j\Delta\tau_2{}^n, \tau_3{}^n+k\Delta\tau_3{}^n)$$
$$i=-1,0,1; \quad j=-1,0,1; \quad k=-1,0,1$$

3) If Error $(i,j,k)<$ Error $(0,0,0)$. Then

$$\tau_1{}^{n+1}=\tau_1{}^n+i\Delta\tau_1{}^n, \tau_2{}^{n+1}=\tau_2{}^n+j\Delta\tau_2{}^n, \tau_3{}^n+1=\tau_3{}^n+k\Delta\tau_3{}^n;$$

Return to Step 2.

4) If error $(i,j,k)\geqq(0,0,0)$, then

$$\Delta\tau_1{}^{n+1}=\Delta\tau_1{}^{n/2}, \quad \Delta\tau_2{}^{n+1}=\Delta\tau_2{}^{n/2}, \quad \Delta\tau_3{}^{n+1}=\Delta\tau_3{}^{n/2}$$

5) If $\Delta\tau_i{}^{n+1}>0.0001$, return to Step 2. If $\Delta\tau_i{}^{n+1}\leqq 0.0001$, STOP.

Analog System

The analog system represents the aircraft with the unknown values of $C_{h\dot{\delta}}$. The analog has the same system equations as Eqs. (2) and (2a). The numerical values of the parameters are the same as those listed in Numerical Example, except for those cases when the parameters are purposely mismatched. The representation for $C_{h\delta}$ is as follows:

$$C_{h\delta}=C_{h\delta 0}\frac{\left(1+j\tau_1'\frac{\omega b}{v}\right)\left(1+j\tau_2'\frac{\omega b}{v}\right)\left(1+j\tau_4'\frac{\omega b}{v}\right)}{\left(1+j\tau_3'\frac{\omega b}{v}\right)\left(1+j\tau_5'\frac{\omega b}{v}\right)}$$

The values for τ' for the numerical examples are

$$t_1'=2.5; \quad \tau_2'=6.0; \quad \tau_3'=10.0; \quad \tau_4'=2.0; \quad \tau_5'=4.0$$

References

[1] Johannes, R. P., "Active Flutter Control Flight Test System Synthesis," Paper 7-B1, *Proceedings of the 12th JACC of the American Automatic Control Council*, 1971, pp. 599–607.

[2] Thompson, G. O. and Kass, G. J., "Active Flutter Suppression—An Emerging Technology," Paper 7-B2, *Proceedings of the 12th JACC of the American Automatic Control Council*, 1971, pp. 608–616.

[3] Topp, L. J., "Potential Performance Gains by Use of A Flutter Suppression System," Paper 7-B3, *Proceedings of the 12th JACC of the American Automatic Control Council*, 1971, pp. 617–623.

[4] Triplett, W. E., "A Feasibility Study of Active Wing/Store Flutter Control," Paper 7-B4, *Proceedings of the 12th JACC of the American Automatic Control Council*, 1971, pp. 624–632.

[5] Theodorsen, T., "General Theory of Aerodynamic Instability and the Mechanism of Flutter," Rept. 496, 1940, NACA.

[6] Garrick, I. E. and Rubinow, S. R., "Flutter and Oscillating Air-Force Calculations for an Airfoil in a Two-Dimensional Supersonic Flow," Rept. 846, 1946, NACA.

[7] Tijdeman, B., "Analysis of Pressure Distributions Measured on a Wing with Oscillating Control Surface in Two-Dimensional High Subsonic and Transonic Flow," NLR-TR F. 253, March 1967, Nationaal Lucht-En Ruimtevaart-Lab., Amsterdam, Netherlands.